Density functional formulation of the random-phase approximation for inhomogeneous fluids: Application to the Gaussian core and Coulomb particles

Derek Frydel
Institute for Advanced Study, Shenzhen University, Shenzhen, Guangdong 518060, China
and School of Chemistry and Chemical Engineering, Shanghai Jiao Tong University, Shanghai 200240, China

Manman Ma
Institute of Natural Sciences, Shanghai Jiao Tong University, Shanghai 200240, China
(Received 20 January 2016; revised manuscript received 8 April 2016; published 7 June 2016)

Using the adiabatic connection, we formulate the free energy in terms of the correlation function of a fictitious system, $h_\lambda(\mathbf{r},\mathbf{r}')$, in which interactions $\lambda u(\mathbf{r},\mathbf{r}')$ are gradually switched on as λ changes from 0 to 1. The function $h_\lambda(\mathbf{r},\mathbf{r}')$ is then obtained from the inhomogeneous Ornstein-Zernike equation and the two equations constitute a general liquid-state framework for treating inhomogeneous fluids. The two equations do not yet constitute a closed set. In the present work we use the closure $c_\lambda(\mathbf{r},\mathbf{r}') \approx -\lambda\beta u(\mathbf{r},\mathbf{r}')$, known as the random-phase approximation (RPA). We demonstrate that the RPA is identical with the variational Gaussian approximation derived within the field-theoretical framework, originally derived and used for charged particles. We apply our generalized RPA approximation to the Gaussian core model and Coulomb charges.

DOI: 10.1103/PhysRevE.93.062112

I. INTRODUCTION

Pair interactions of hard-sphere fluids derive from the excluded volume effects: Non-overlapping configurations recover an ideal-gas behavior, but the exclusion of overlapping configurations reduces available phase space, leading at high density to phase transition. In this sense, the hard-sphere fluids constitute a geometric problem. Within various successful (nonlocal) density-functional theories (DFT), a free-energy functional for hard-sphere fluids is built from a weighted rather than local density—nonlocality is attained by construction [1]. In early prescriptions, a weighted density corresponded to a convoluted local density, where the single convoluting function was the Mayer f function. The resulting theories and their refinements and extensions came to be known as the weighted DFT theories. A crucial next development was to decompose a Mayer f function into several weight functions, yielding multiple weighted densities and, by the same token, multiple building blocks from which an approximate $F_{\rm ex}$ was to be constructed [2–6]. Referred to as the fundamental measure (FM) DFT, a nice feature of this approach is the capture of a correct dimensional crossover: Each consecutive reduction of the system dimensionality, 3D $\to$ 2D $\to$ 1D $\to$ 0D, recovers either an accurate or exact $F_{\rm ex}$.

The success of the hard-sphere DFT theories (and the lack of equivalent theories for arbitrary pair interactions) prompted attempts to implement the hard-sphere framework to other types of short-range interactions. It became something of a standard method to map particles with arbitrary short-range interactions onto a hard-sphere fluid by ascribing to a pair potential of interest an effective diameter. Density profiles are then obtained from a (hard-sphere) DFT theory of choice. The Barker-Henderson effective diameter is one recipe among others for extracting an effective diameter [7].

A more sophisticated example is the "soft" fundamental measure DFT, developed for penetrable spheres (spheres may overlap but at an energy cost). Within this method $F_{\rm ex}$ is constructed to satisfy a correct dimensional crossover [8–12].

But for particles with arbitrary pair interactions, where excluded volume effects are not dominant, the mean-field approximation is still a preferred theoretical tool [13–17]. An important example are charged particles with long-range interactions. Another example are penetrable particles with bounded (nondivergent) interactions, such as the Gaussian core model or the already-mentioned penetrable spheres. But the correlations neglected by the mean-field description are not always trivial. This is particularly true of Coulomb systems. In such a case the "beyond-mean-field" approach is desirable. Splitting the excess free energy into the mean-field and correlation contribution, $F_{\rm ex}[\rho] = \frac{1}{2}\int d\mathbf{r}\int d\mathbf{r}'\,\rho(\mathbf{r})\rho(\mathbf{r}')u(\mathbf{r},\mathbf{r}') + F_c[\rho]$, where $\rho(\mathbf{r})$ is a number density and $u(\mathbf{r},\mathbf{r}')$ is an arbitrary pair interaction, the "beyond-mean-field" approach amounts to finding an appropriate functional $F_c[\rho]$.

The "beyond-mean-field" approximations for Coulomb systems are dominantly formulated within the field-theoretical framework based on mathematical transformation of a partition function, using a Gaussian integral identity [18], into a functional integral over an auxiliary fluctuating field [18–26]. The saddle point of the effective Hamiltonian recovers the mean-field solution, while the harmonic fluctuations around the saddle point account for weak (Gaussian) correlations. If formulated variationally, the Gaussian approximation become self-consistent (nonperturbative) and is deemed superior to the perturbative formulation [18,23,24]. The primary drawback of the field-theoretical formulation is its unintuitiveness by adapting an auxiliary phase space.

In this work we lay out a general density functional framework of inhomogeneous fluids. We then specifically use the random-phase approximation closure (RPA). It turns out that the Gaussian approximation is equivalent to the well-established random phase approximation (RPA) [27], a mathematical signature of which is its being composed of an infinite summation of ring diagrams [28]. In hindsight, this is not so entirely surprising to find the connection between the harmonic fluctuations of an auxiliary field around the saddle point and the density functional formulation of the

RPA. To our knowledge, this connection, so far, has not been formally established. The liquid-state formulation of the RPA of this work is general and in principle applicable to any pair interactions, not just Coulomb particles. In this sense we generalize the RPA not just to inhomogeneous fluids but to all particles.

In Sec. II we formulate the free energy within the liquid-state formalism using the adiabatic connection. By coupling it to the OZ equation, we set up a general theoretical framework for inhomogeneous fluids. In Sec. III, using specifically the RPA closure, we derive the appropriate self-consistent equations. In Sec. IV we generalize the equations to multiple species. Finally, in Secs. V, VII, and VIII we test the RPA approximation on concrete systems with wall geometry.

II. ADIABATIC CONNECTION FORMULATION OF THE FREE ENERGY

Given a general Hamiltonian for a system of interacting particles,

$$H = \sum_{i=1}^{N} U(\mathbf{r}_i) + \frac{1}{2}\sum_{i\neq j}^{N} u(\mathbf{r}_i,\mathbf{r}_j), \tag{1}$$

where $U(\mathbf{r})$ is an external potential, $u(\mathbf{r},\mathbf{r}')$ is a pair interaction, and N is the number of particles, our aim is to obtain a free-energy expression in terms of physically meaningul quantities. To this end, we use the adiabatic connection route [29,30], wherein interactions are gradually switched on within a fictitious λ-dependent system,

$$H_\lambda = \sum_{i=1}^{N} U_\lambda(\mathbf{r}_i) + \frac{\lambda}{2}\sum_{i\neq j}^{N} u(\mathbf{r}_i,\mathbf{r}_j), \tag{2}$$

where the λ-dependent external potential $U_\lambda(\mathbf{r})$ is introduced to keep a density fixed at its physical value for all λ, and the value $\lambda = 1$ recovers the physical potential, $U_{\lambda=1}(\mathbf{r}) = U(\mathbf{r})$.

The partition function and the free energy of a fictitious system are

$$Z_\lambda = \int d\mathbf{r}_1 \ldots \int d\mathbf{r}_N\, e^{-\beta H_\lambda} \tag{3}$$

and

$$\beta F_\lambda = -\log Z_\lambda, \tag{4}$$

respectively. The free energy of a physical system can be expressed in terms of a fictitious system, as a thermodynamic integration,

$$F = F_0 + \int_0^1 d\lambda\, \frac{\partial F_\lambda}{\partial \lambda}, \tag{5}$$

where the reference free energy is

$$F_0[\rho] = F_{\rm id}[\rho] + \int d\mathbf{r}\, \rho(\mathbf{r}) U_{\lambda=0}(\mathbf{r}), \tag{6}$$

and

$$F_{\rm id}[\rho] = k_B T \int d\mathbf{r}\, \rho(\mathbf{r})[\log \rho(\mathbf{r})\Lambda^3 - 1] \tag{7}$$

is an ideal-gas free energy. The integrand in Eq. (5) can be written as

$$\frac{\partial F_\lambda}{\partial \lambda} = \int d\mathbf{r}\, \rho(\mathbf{r}) \frac{\partial U_\lambda(\mathbf{r})}{\partial \lambda} + \frac{1}{2}\int d\mathbf{r} \int d\mathbf{r}'\, \rho(\mathbf{r})\rho(\mathbf{r}')u(\mathbf{r},\mathbf{r}') + \frac{1}{2}\int d\mathbf{r} \int d\mathbf{r}'\, \rho(\mathbf{r})\rho(\mathbf{r}')h_\lambda(\mathbf{r},\mathbf{r}')u(\mathbf{r},\mathbf{r}') \tag{8}$$

and Eq. (5) becomes

$$\begin{aligned} F[\rho] = F_{\rm id}[\rho] &+ \int d\mathbf{r}\, \rho(\mathbf{r}) U_{\lambda=0}(\mathbf{r}) \\ &+ \int_0^1 d\lambda \int d\mathbf{r}\, \rho(\mathbf{r}) \frac{\partial U_\lambda(\mathbf{r})}{\partial \lambda} \\ &+ \frac{1}{2}\int d\mathbf{r} \int d\mathbf{r}'\, \rho(\mathbf{r})\rho(\mathbf{r}')u(\mathbf{r},\mathbf{r}') \\ &+ \frac{1}{2}\int d\mathbf{r} \int d\mathbf{r}'\, \rho(\mathbf{r})\rho(\mathbf{r}')u(\mathbf{r},\mathbf{r}') \int_0^1 d\lambda\, h_\lambda(\mathbf{r},\mathbf{r}'). \end{aligned} \tag{9}$$

After a number of cancelations we arrive at the final form,

$$\begin{aligned} F[\rho] = F_{\rm id}[\rho] &+ \int d\mathbf{r}\, \rho(\mathbf{r}) U(\mathbf{r}) \\ &+ \frac{1}{2}\int d\mathbf{r} \int d\mathbf{r}'\, \rho(\mathbf{r})\rho(\mathbf{r}')u(\mathbf{r},\mathbf{r}') \\ &+ \frac{1}{2}\int d\mathbf{r} \int d\mathbf{r}'\, \rho(\mathbf{r})\rho(\mathbf{r}')u(\mathbf{r},\mathbf{r}') \int_0^1 d\lambda\, h_\lambda(\mathbf{r},\mathbf{r}'). \end{aligned} \tag{10}$$

[A similar expression has been derived in Ref. [31] in Eq. (3.4.10).] Note that the final expression does not depend on the fictitious potential U_λ. The only quantity that depends on λ is a correlation function $h_\lambda(\mathbf{r},\mathbf{r}')$. The first three terms of Eq. (10) constitute the mean-field approximation,

$$F_{\rm mf} = F_{\rm id} + \int d\mathbf{r}\, \rho(\mathbf{r})U(\mathbf{r}) + \frac{1}{2}\int d\mathbf{r} \int d\mathbf{r}'\, \rho(\mathbf{r})\rho(\mathbf{r}')u(\mathbf{r},\mathbf{r}'), \tag{11}$$

and the last term is the correlation free energy,

$$F_c = \frac{1}{2}\int_0^1 d\lambda \int d\mathbf{r}\, \rho(\mathbf{r}) \left[\int d\mathbf{r}'\, \rho(\mathbf{r}')h_\lambda(\mathbf{r},\mathbf{r}')u(\mathbf{r},\mathbf{r}') \right]. \tag{12}$$

Not surprisingly, F_c depends on the correlation function $h_\lambda(\mathbf{r},\mathbf{r}')$ that is obtained from the Ornstein-Zernike equation (OZ),

$$h_\lambda(\mathbf{r},\mathbf{r}') = c_\lambda(\mathbf{r},\mathbf{r}') + \int d\mathbf{r}''\, \rho(\mathbf{r}'')h_\lambda(\mathbf{r}',\mathbf{r}'')c_\lambda(\mathbf{r},\mathbf{r}''), \tag{13}$$

a standard relation within the liquid-state theory that expresses the correlation function in terms of the direct correlation function $c_\lambda(\mathbf{r},\mathbf{r}')$. The introduction of $c_\lambda(\mathbf{r},\mathbf{r}')$ requires additional closure to complete an approximation.

III. RANDOM-PHASE APPROXIMATION

We consider the simplest closure available,

$$c_\lambda(\mathbf{r},\mathbf{r}') = -\beta\lambda u(\mathbf{r},\mathbf{r}'), \tag{14}$$

known as the RPA. The closure modifies the exact Ornstein-Zernike relation in Eq. (13),

$$h_\lambda(\mathbf{r},\mathbf{r}') = -\beta\lambda u(\mathbf{r},\mathbf{r}') - \beta\lambda \int d\mathbf{r}''\rho(\mathbf{r}'')h_\lambda(\mathbf{r}',\mathbf{r}'')u(\mathbf{r},\mathbf{r}''). \tag{15}$$

Accordingly, we refer to it as the OZ-RPA equation. Application of the OZ-RPA modifies the correlation free energy in Eq. (12),

$$F_c[\rho] = -\frac{1}{2}\int d\mathbf{r}\rho(\mathbf{r})\int_0^1 d\lambda\,\frac{h_\lambda(\mathbf{r},\mathbf{r})}{\lambda\beta} - \frac{u(0)}{2}\int d\mathbf{r}\,\rho(\mathbf{r}). \tag{16}$$

In the above equation $u(0) = u(\mathbf{r},\mathbf{r})$. Likewise, for homogeneous fluids in a bulk we write $h_b(0) = h_b(\mathbf{r},\mathbf{r})$.

A. Connection with the field-theoretical formulation

The λ dependence in F_c can be eliminated by expanding $h_\lambda(\mathbf{r},\mathbf{r}')$,

$$\begin{aligned} h_\lambda(\mathbf{r},\mathbf{r}') = &-\beta\lambda u(\mathbf{r},\mathbf{r}') + \beta^2\lambda^2\int d\mathbf{r}_1\,\rho(\mathbf{r}_1)u(\mathbf{r},\mathbf{r}_1)u(\mathbf{r}_1,\mathbf{r}') \\ &-\beta^3\lambda^3\int d\mathbf{r}_1\int d\mathbf{r}_2\,\rho(\mathbf{r}_1)\rho(\mathbf{r}_2) \\ &\times u(\mathbf{r},\mathbf{r}_1)u(\mathbf{r}_1,\mathbf{r}_2)u(\mathbf{r}_2,\mathbf{r}') + \ldots \end{aligned} \tag{17}$$

The expansion is generated iteratively by repeated insertion of the right-hand side of Eq. (15) for every occurrence of $h_\lambda(\mathbf{r},\mathbf{r}')$. The formulas are simplified by introducing an operator,

$$A(\mathbf{r},\mathbf{r}') = \beta\rho(\mathbf{r})u(\mathbf{r},\mathbf{r}'), \tag{18}$$

and adopting a convention,

$$A^n = \int d\mathbf{r}_1\int d\mathbf{r}_2\ldots\int d\mathbf{r}_{n-1}A(\mathbf{r},\mathbf{r}_1)A(\mathbf{r}_1,\mathbf{r}_2)\ldots A(\mathbf{r}_{n-1},\mathbf{r}'), \tag{19}$$

by means of which we get

$$\begin{aligned} \rho(\mathbf{r})h_\lambda(\mathbf{r},\mathbf{r}') &= -\lambda A + \lambda^2A^2 - \lambda^3A^3 + \ldots \\ &= -\left(\frac{\lambda A}{I+\lambda A}\right), \end{aligned} \tag{20}$$

where $I = \delta(\mathbf{r},\mathbf{r}')$ is the identity matrix in the continuum limit. Integration over λ now is done explicitly,

$$\begin{aligned} \int_0^1 d\lambda\,\frac{\rho(\mathbf{r})h_\lambda(\mathbf{r},\mathbf{r}')}{\lambda} &= -A + \frac{A^2}{2} - \frac{A^3}{3} + \ldots \\ &= -\log[I+A], \end{aligned} \tag{21}$$

and $F_c[\rho]$ becomes

$$F_c[\rho] = \frac{k_BT}{2}\mathrm{Tr}\,\log[I+A] - \frac{u(0)}{2}\int d\mathbf{r}\,\rho(\mathbf{r}), \tag{22}$$

where the first term yields an infinite series of ring diagrams, a characteristic feature of the RPA.

The expression can further be rearranged by using the formal matrix identity,

$$\frac{1}{2}\mathrm{Tr}\,\log[I+A] = \log\sqrt{\det\left[I+A\right]}, \tag{23}$$

and the fact that a functional determinant is a solution of a Gaussian functional integral,

$$\frac{1}{\sqrt{\det\left[I+A\right]}} = \int \mathcal{D}\phi\, e^{-\frac{1}{2}\int d\mathbf{r}\int d\mathbf{r}'\,\phi(\mathbf{r})\phi(\mathbf{r}')[\delta(\mathbf{r}-\mathbf{r}')+A(\mathbf{r},\mathbf{r}')]}, \tag{24}$$

where $\phi(\mathbf{r})$ is a fluctuating field and $\int\mathcal{D}\phi$ is a functional integral. The partition function within the RPA can now be written as a Gaussian functional integral,

$$\begin{aligned} Z_{\mathrm{rpa}} = &\, e^{\frac{\beta N}{2}u(0)}e^{-\beta F_{\mathrm{mf}}} \\ &\times\int\mathcal{D}\phi\, e^{-\frac{1}{2}\int d\mathbf{r}\int d\mathbf{r}'\,\phi(\mathbf{r})\phi(\mathbf{r}')[\delta(\mathbf{r}-\mathbf{r}')+A(\mathbf{r},\mathbf{r}')]}, \end{aligned} \tag{25}$$

where we used $F = F_{\mathrm{mf}} + F_c$ and $Z = e^{-\beta F_{\mathrm{mf}}}e^{-\beta F_c}$.

In consequence, we propose an alternative, liquid-state route to generate the functional integral formulation of the free energy without resorting to the Hubbard-Stratonovich transformation. By adapting the density functional approach we avoid a number of artifacts arising in the field-theoretical formalism, such as the problem of divergences, or inapplicability of the Gibbs-Bogolyubov-Feynman inequality to complex functions when constructing variational equations [18].

B. Density profile

To obtain an equilibrium density we use the known thermodynamic condition,

$$\frac{\delta F}{\delta\rho(\mathbf{r})} = \mu, \tag{26}$$

where μ denotes the chemical potential. The functional derivative of F_c with respect to $\rho(\mathbf{r})$ incidentally eliminates all λ dependence,

$$\begin{aligned} \frac{\delta F_c}{\delta\rho(\mathbf{r})} &= \frac{k_BT}{2}\frac{\delta\mathrm{Tr}\,\log[I+A]}{\delta\rho(\mathbf{r})} - \frac{1}{2}u(0) \\ &= -\frac{1}{2}[u(0) + k_BTh(\mathbf{r},\mathbf{r})], \end{aligned} \tag{27}$$

and the functional derivative is written in terms of a correlation function of a physical system, $h(\mathbf{r},\mathbf{r})$ [this is better seen in conjunction with Eq. (21) and Eq. (17)]. The number density that results is

$$\rho(\mathbf{r}) = \rho_b e^{-\beta U(\mathbf{r})}e^{-\beta\int d\mathbf{r}'\,\rho(\mathbf{r}')u(\mathbf{r},\mathbf{r}')}e^{\frac{1}{2}[\beta u(0)+h(\mathbf{r},\mathbf{r})]+\beta\mu_{\mathrm{ex}}}, \tag{28}$$

where we separated a chemical potential into ideal and excess parts, $\mu = \mu_{\mathrm{id}} + \mu_{\mathrm{ex}}$, with the ideal contribution related to a bulk density,

$$\rho_b = \left(\frac{e^{\beta\mu_{\mathrm{id}}}}{\Lambda^3}\right). \tag{29}$$

The excess chemical potential within the present approximation is

$$\mu_{\mathrm{ex}} = \rho_b\int d\mathbf{r}\,u(r) - \frac{1}{2}[u(0) + k_BTh_b(0)], \tag{30}$$

where $h_b(r)$ is a correlation function in a bulk. For $U(\mathbf{r}) = 0$, we accurately recover a bulk density, $\rho(\mathbf{r}) \to \rho_b$. More conveniently, a density can be written as

$$\rho(\mathbf{r}) = \rho_b e^{-\beta U(\mathbf{r})}e^{-\beta\int d\mathbf{r}'\,(\rho(\mathbf{r}')-\rho_b)u(\mathbf{r},\mathbf{r}')}e^{\frac{1}{2}[h(\mathbf{r},\mathbf{r})-h_b(0)]}. \tag{31}$$

C. Direct correlation function

In constructing the generalized RPA framework (GRPA) we used the closure $c(\mathbf{r},\mathbf{r}') = -\beta u(\mathbf{r},\mathbf{r}')$. Using the formal definition of the direct correlation function within the resulting GRPA framework, we find

$$c(\mathbf{r},\mathbf{r}') = -\frac{\delta^2 \beta F_{\rm ex}}{\delta\rho(\mathbf{r})\delta\rho(\mathbf{r}')} = -\beta u(\mathbf{r},\mathbf{r}') + \frac{1}{2}\frac{\delta h(\mathbf{r},\mathbf{r})}{\delta\rho(\mathbf{r}')}$$
$$= -\beta u(\mathbf{r},\mathbf{r}')\left(1 + \frac{1}{2}\frac{\partial h_\lambda(\mathbf{r},\mathbf{r}')}{\partial\lambda}\bigg|_{\lambda=1}\right), \tag{32}$$

which yields an additional term, absent in the standard RPA [13,32]. For homogeneous fluids this reduces to

$$c(r) = -\beta u(r)\left(1 + \frac{1}{2}\frac{\partial h_\lambda(r)}{\partial\lambda}\bigg|_{\lambda=1}\right)$$
$$= -\beta u(r)\left(1 + \frac{1}{2}\frac{\partial \rho_b h(r)}{\partial\rho_b}\right). \tag{33}$$

Note that a number of expressions of the GRPA approximation include the term $u(0)$, which may lead to assumption that the RPA is inappropriate for divergent pair interactions. A careful inspection, however, shows that the divergence in $u(\mathbf{r},\mathbf{r}')$ is always canceled by another divergence in $h(\mathbf{r},\mathbf{r}')$ [see the expansion in Eq. (17)]. The true pair correlation function, however, never diverges as $\mathbf{r}' \to \mathbf{r}$ and the lower bound is given as $h(\mathbf{r},\mathbf{r}') > -1$ and indicates the exclusion of a particle from the position $\mathbf{r}$ if another particle is at $\mathbf{r}'$. The divergence in $h(\mathbf{r},\mathbf{r}')$ is, therefore, an artifact of the GRPA that is essential for keeping the GRPA expressions well behaved.

D. Pressure and the contact value theorem

Pressure is obtainable from a number of definitions. From the "compressibility" route we get

$$P_{\rm ex} = P - k_B T\rho_b = \int_0^{\rho_b} d\rho\, \rho \frac{\partial \mu_{\rm ex}}{\partial\rho}, \tag{34}$$

where we use Eq. (30) for $\mu_{\rm ex}$ and get

$$P_{\rm ex} = \frac{\rho_b^2}{2}\int d\mathbf{r}\, u(r) - \frac{k_B T}{2}\int_0^{\rho_b} d\rho\, \rho \frac{\partial h_b(0)}{\partial\rho}. \tag{35}$$

[The "compressibility" expression can also be defined as $P_{\rm ex} = -k_B T \int d\mathbf{r} \int_0^{\rho_b} d\rho\, \rho\, c(r)$, where $c(r)$ in Eq. (33) yields the same answer]. Alternatively, the pressure is defined through a "virial" route,

$$P_{\rm ex} = \frac{\rho_b^2}{2}\int d\mathbf{r}\, u(r) - \frac{\rho_b^2}{6}\int d\mathbf{r}\, h(r)\, r\frac{\partial u(r)}{\partial r}. \tag{36}$$

Within a consistent approximation the "virial" and "compressibility" expressions yield the same result. In order to compare the two expressions, we introduce a particle scaling by assuming a general potential form, $\beta u(r) = \varepsilon f(r/\sigma)$. Using the identity $r\frac{\partial u(r)}{\partial r} = -\sigma\frac{\partial u(r)}{\partial\sigma}$ and the fact that a particle scaling is similar to density variation, and working with the expansion in Eq. (17), it can be demonstrated after some manipulation that

$$\frac{\rho_b^2}{6}\int d\mathbf{r}\, h(r)\, r\frac{\partial u(r)}{\partial r} = \frac{k_B T}{2}\int_0^{\rho_b} d\rho\, \rho\frac{\partial h_b(0)}{\partial\rho}, \tag{37}$$

and the "virial" and "compressibility" routes within the GRPA lead to the same result.

(There are a number of ways to express thermodynamic integrals such as

$$\int_0^{\rho_b} d\rho\, \rho\frac{\partial h_b(0)}{\partial\rho} = \rho_b\int_0^1 d\lambda\, \lambda\frac{\partial\left(h_b^\lambda(0)/\lambda\right)}{\partial\lambda}$$
$$= {\rm Tr}\left(\log[I+A] - \frac{A}{I+A}\right). \tag{38}$$

The advantage of integration is that it represents a physical process that is easy to conceive, such as "charging," or a gradual increase of density. But from mathematical point of view, integration modifies coefficients of an expansion in the operator $A = \rho_b\beta u(\mathbf{r},\mathbf{r}')$. The terms A^n constitute the true building blocks of the GRPA approximation).

Alternatively, pressure, can be obtained not from bulk parameters but from a density profile of a fluid confined by a planar hard wall. Fluid itself is in contact with a reservoir and a density profile somehow "knows" what the reservoir thermodynamic parameters are. According to the contact value theorem sum rule, the pressure is related to a value of a density profile directly at a wall, ρ_w,

$$P = k_B T\rho_w, \tag{39}$$

and the excess pressure according to the contact value sum rule is

$$P_{\rm ex} = k_B T(\rho_w - \rho_b) \tag{40}$$

We first demonstrate that the contact value theorem sum rule is satisfied by the mean-field. The excess pressure in terms of bulk quantities, obtained from either "compressibility" or "virial" route, is

$$P_{\rm ex} = \frac{\alpha\rho_b^2}{2}, \tag{41}$$

where we use $\alpha = \int d\mathbf{r}\, u(r)$ to reduce the notation. To demonstrate that the contact value theorem relation is satisfied, we need to prove the following equivalence:

$$k_B T(\rho_w - \rho_b) = \frac{\alpha\rho_b^2}{2}, \tag{42}$$

which needs to be obtained from the mean-field density alone,

$$\rho(x) = \rho_b e^{-\beta\int_0^\infty dx'\,\rho(x')u(x,x')} e^{\beta\alpha\rho_b}, \tag{43}$$

assuming that the planar hard wall is at $x = 0$, and where we used

$$u(x,x') = 2\pi\int_0^\infty dR\, R\, u(\mathbf{r},\mathbf{r}'), \tag{44}$$

where (R,ϕ,x) are cylindrical coordinates with the angle ϕ integrated out. We proceed by differentiating both sides,

$$\frac{d\rho(x)}{dx} = -\beta\rho(x)\int_0^\infty dx'\,\rho(x')\frac{du(x,x')}{dx}, \tag{45}$$

then we integrate the expression inside the interval $[0^+,L]$ (excluding the wall at $x = 0$), where L is finite but considerably larger than all other length scales, so $\rho(L) = \rho_b$, and we get

$$k_B T(\rho_w - \rho_b) = \int_0^L dx\,\rho(x)\int_0^\infty dx'\,\rho(x')\frac{du(x,x')}{dx}. \tag{46}$$

In order to prove the contact value theorem sum rule, we need somehow to show that the integral on the right-hand side, which depends on a nonuniform density profile near a wall, can be related to the bulk, or reservoir thermodynamic parameters, by somehow moving the integration limits from the vicinity of the wall far into a bulk where the density is uniform. To do this it helps to understand what this integral represents physically. By recognizing $F(x,x') = -\frac{du(x,x')}{dx}$ as force exerted by a particle at x' on a particle at x, and rewriting the integration limits of the right-hand side term as

$$\int_0^L dx\, \rho(x) \int_0^{L+\infty} dx'\, \rho(x') \frac{du(x,x')}{dx}, \tag{47}$$

and noting that

$$\int_0^L dx\, \rho(x) \int_0^L dx'\, \rho(x') \frac{du(x,x')}{dx} = 0, \tag{48}$$

which is true for any $\rho(x)$ since $du(x,x')/dx = -du(x,x')/dx'$ so that the total net force vanishes (particles exert on each other the same but opposite force), then the right-hand term in Eq. (46) becomes

$$\begin{aligned} k_B T(\rho_w - \rho_b) &= \int_0^L dx\, \rho(x) \int_L^\infty dx'\, \rho(x') \frac{du(x,x')}{dx} \\ &= -\int_0^L dx\, \rho(x) \int_L^\infty dx'\, \rho(x') \frac{du(x,x')}{dx'} \\ &= \rho_b \int_0^L dx\, \rho(x)[u(x,L) - u(x,\infty)] \\ &= \rho_b^2 \int_0^L dx\, u(x,L) = \frac{\alpha \rho_b^2}{2}, \end{aligned} \tag{49}$$

and indeed Eq. (42) has been confirmed and the consistency of the contact value theorem for the mean-field proved. The one-half factor in the result reflects the fact that the integration was carried out inside a half-space.

Note that the integral term on the right-hand side of Eq. (49) represents a force between two sections of a fluid separated by an invisible wall at $x = L$. Since L can be placed arbitrarily far from the wall, the contributions of nonuniform density near a wall can easily be neglected, and the resulting integral represents a force per unit area between two uniform fluids brought into direct contact along an infinite plane.

Note that Eq. (48) is true for any profile $\rho(x)$, as long as it converges to a bulk value far from the wall. This introduces only a weak constraint and we could insert into Eq. (45) the simplest possible density profile, $\rho(x) = \rho_b \theta(x)$ [where $\theta(x)$ is the Heaviside step function], which itself does not satisfy the contact value sum rule but which yields the same result as that in Eq. (49) and that simplifies the calculations.

A similar proof needs to be carried out for the GRPA, except now one needs to prove

$$k_B T(\rho_w - \rho_b) = \frac{\alpha \rho_b^2}{2} - \frac{k_B T \rho_b}{2} \int_0^1 d\lambda\, \lambda \frac{\partial \left(h_b^\lambda(0)/\lambda\right)}{\partial \lambda} \tag{50}$$

from the density profile

$$\rho(x) = \rho_b e^{-\beta \int_0^\infty dx'\, \rho(x') u(x,x')} e^{h(x,x)/2} e^{\beta \alpha \rho_b - h_b(0)/2} \tag{51}$$

with a confining wall at $x = 0$. We proceed in the same fashion as for the mean-field. Performing differentiation followed by integration within the interval $[0^+, L]$ we find

$$k_B T(\rho_w - \rho_b) = \frac{\alpha \rho_b^2}{2} - \frac{k_B T}{2} \int_0^L dx\, \rho(x) \frac{dh(x,x)}{dx}, \tag{52}$$

where the first (mean-field) term does not change, being independent of details of a density profile. To evaluate the integral term, we again want to move the integration limits away from a wall. To be able to do this, we expand the correlation function using Eq. (17) to get

$$\begin{aligned} \int_0^L dx\, \rho(x) \frac{dh(x,x)}{dx} &= \beta^2 \int_0^L dx\, \rho(x) \int_0^{L+\infty} dx'\, \rho(x') \frac{du^2(x,x')}{dx} \\ &\quad -\beta^3 \int_0^L dx\, \rho(x) \int_0^{L+\infty} d\mathbf{r}'\, \rho(x') \\ &\quad \times \int_0^{L+\infty} d\mathbf{r}''\, \rho(x'') \frac{d}{dx} w(\mathbf{r},\mathbf{r}',\mathbf{r}'') + \ldots \end{aligned} \tag{53}$$

We consider the first two terms and check that they agree with the initial terms from either "virial" or "compressibility" expressions. The function

$$w(\mathbf{r},\mathbf{r}',\mathbf{r}'') = u(\mathbf{r},\mathbf{r}')u(\mathbf{r}',\mathbf{r}'')u(\mathbf{r}'',\mathbf{r}) \tag{54}$$

plays the role of a three-body potential. This interpretation will allow us to shift the integration limits away from the wall. The first integral is similar to the mean-field case except that the two-body potential now is $u^2(\mathbf{r},\mathbf{r}')$. The second term requires considerable elaboration and we only show the end result,

$$\begin{aligned} \int_0^L dx\, \rho(x) \frac{dh(x,x)}{dx} &= \frac{1}{2}\beta^2 \rho_b^2 \int d\mathbf{r} \int d\mathbf{r}' u^2(\mathbf{r},\mathbf{r}') \\ &\quad -\frac{2}{3}\beta^3 \rho_b^3 \int d\mathbf{r} \int d\mathbf{r}' \int d\mathbf{r}''\, u(\mathbf{r},\mathbf{r}')u(\mathbf{r}',\mathbf{r}'') \\ &\quad \times u(\mathbf{r}'',\mathbf{r}) + \ldots \\ &= \frac{1}{2}\mathrm{Tr}\, A^2 - \frac{2}{3}\mathrm{Tr}\, A^3 + \ldots \end{aligned} \tag{55}$$

and the initial terms are in agreement with those in Eq. (38). We conclude, to the credit of the approximation, that the GRPA satisfies the contact value theorem and consistently predicts the same pressure independent of route.

As for the case of the mean-field, the value of the integral in Eq. (55) is independent of a density profile, as long that profile falls off to a bulk value. This weak constraint permits us to assume the simple profile $\rho(x) = \rho_b \theta(x)$ which yields

$$\int_0^L dx\, \rho(x) \frac{dh(x,x)}{dx} = \rho_b h_b(0) - \rho_b h_w(0). \tag{56}$$

However, the substitution does not provide a straightforward answer we might have hoped for. The evaluation of the correlation function at the edge of a half-space, $h_w(0)$, is also quite complicated as each term in the expansion in Eq. (17) needs to be evaluated separately. This essentially constitutes a geometric problem of determining how the removal of a half-space at $x < 0$ effects the correlation function. Incidentally, this also provides an explanation to the question of why local

approximations fail in satisfying the contact value theorem. For the density profile $\rho(x) = \rho_b\theta(x)$ all quantities (being local) are the same regardless if they are evaluated near or far from an interface, in which case $h_w(0) = h_b(0)$.

E. Dilute limit

The pair correlation function in the dilute limit is

$$h_\lambda(\mathbf{r},\mathbf{r}') \approx e^{-\beta\lambda u(\mathbf{r},\mathbf{r}')} - 1 \tag{57}$$

and is obtained by fixing a single particle at $\mathbf{r}'$ and determining the distribution of mobile particles by treating them as ideal gas particles. On the other hand, the dilute limit of the GRPA yields $h(\mathbf{r},\mathbf{r}') \approx c(\mathbf{r},\mathbf{r}')$

$$h_\lambda(\mathbf{r},\mathbf{r}') \approx -\beta\lambda u(\mathbf{r},\mathbf{r}'), \tag{58}$$

see Eq. (17). The two expressions agree only in the high-temperature limit. The problem seems to originate in the very assumption of the RPA, $c(\mathbf{r},\mathbf{r}') = -\beta u(\mathbf{r},\mathbf{r}')$.

The failure of the RPA in the low-density and low-temperature limit is attested to by other quantities. We consider the excess chemical potential and excess pressure,

$$\mu_{\rm ex} = \rho_b \int d\mathbf{r}\, u(r)\left(1 - \frac{\beta}{2}u(r)\right) + O\left(\rho_b^2\right), \tag{59}$$

$$P_{\rm ex} = \frac{\rho_b^2}{2}\int d\mathbf{r}\, u(r)\left(1 - \frac{\beta}{2}u(r)\right) + O\left(\rho_b^3\right), \tag{60}$$

respectively. At low temperature, the RPA chemical potential and excess pressure become negative even for repulsive interactions. This instability is not reproduced by exact results. Since pressure is related to the value of a density profile at a contact with a wall, it is inferred that the density profile must be poorly approximated as well. The conclusion is that the GRPA constitutes a correction to the mean-field, but, like the mean-field, it becomes more accurate for dense fluids, where a large number of particle overlaps justifies the mean-field point of view.

IV. MULTIPLE SPECIES

Next we generalize the RPA to multiple species. The fictitious Hamiltonian, equivalent to that in Eq. (1), is

$$H_\lambda = \sum_{i=1}^{N} U_i^\lambda(\mathbf{r}_i) + \frac{\lambda}{2}\sum_{i\neq j}^{N} u_{ij}(\mathbf{r}_i,\mathbf{r}_j). \tag{61}$$

Here we assume that each particle feels different external potential, and pair interactions between different pairs differ. Of course, particles do not all differ but generally are grouped into species.

Assuming K different species, the free energy from the adiabatic connection is

$$F[\{\rho_k\}] = F_{\rm id}[\{\rho_k\}] + \sum_{k=1}^{K}\int d\mathbf{r}\, U_k(\mathbf{r})\rho_k(\mathbf{r}) + \frac{1}{2}\sum_{k,l}^{K}\int d\mathbf{r}\int d\mathbf{r}'\, \rho_k(\mathbf{r})\rho_l(\mathbf{r}')u_{kl}(\mathbf{r},\mathbf{r}') + \frac{1}{2}\sum_{k,l}^{K}\int d\mathbf{r}\int d\mathbf{r}'\, \rho_k(\mathbf{r})\rho_l(\mathbf{r}')u_{kl}(\mathbf{r},\mathbf{r}') \times \int_0^1 d\lambda\, h_{kl}^\lambda(\mathbf{r},\mathbf{r}'), \tag{62}$$

where the ideal-gas contribution is

$$\beta F_{\rm id}[\{\rho_k\}] = \sum_{i=1}^{K}\int d\mathbf{r}\,\rho_k(\mathbf{r})[\log\rho_k(\mathbf{r})\Lambda^3 - 1]. \tag{63}$$

If the Ornstein-Zernike equation of a multiple-species fluid is

$$h_{kl}^\lambda(\mathbf{r},\mathbf{r}') = c_{kl}^\lambda(\mathbf{r},\mathbf{r}') + \sum_{n=1}^{K}\int d\mathbf{r}''\rho_n(\mathbf{r}'')h_{nl}^\lambda(\mathbf{r}',\mathbf{r}'')c_{kn}^\lambda(\mathbf{r}'',\mathbf{r}), \tag{64}$$

where correlations between particles of a species k and l are mediated by all particles disregarding their type, then the RPA closure, $c_{kl}^\lambda = \beta\lambda u_{kl}(\mathbf{r},\mathbf{r}')$, yields

$$h_{kl}^\lambda(\mathbf{r},\mathbf{r}') = -\beta\lambda u_{kl}(\mathbf{r},\mathbf{r}') - \beta\lambda\sum_{n}\int d\mathbf{r}''\rho_n(\mathbf{r}'')h_{nl}^\lambda(\mathbf{r}',\mathbf{r}'')u_{kn}(\mathbf{r}'',\mathbf{r}), \tag{65}$$

and the RPA correlation free energy is

$$F_c = -\frac{1}{2}\sum_{k=1}^{K}u_{kk}(0)\int d\mathbf{r}\,\rho_k(\mathbf{r}) - \frac{1}{2}\sum_{k=1}^{K}\int d\mathbf{r}\,\rho_k(\mathbf{r})\int_0^1 d\lambda\,\frac{h_{kk}^\lambda(\mathbf{r},\mathbf{r})}{\beta\lambda}. \tag{66}$$

[Compare with Eq. (16) for a one component system.] The lack of dependence on inter-species correlations, that is, $h_{kl}(\mathbf{r},\mathbf{r}')$ for $k \neq l$, at first glance appears inaccurate. But as correlations between particles of the same species, $h_{kk}(\mathbf{r},\mathbf{r}')$, are mediated by all particles disregarding their type, the cross-correlations are always implicit in $h_{kk}(\mathbf{r},\mathbf{r}')$.

A. Density

As for a one-species system, an equilibrium density of a species k of a multiple-species fluid is obtained from the condition

$$\frac{\delta F}{\delta\rho_k(\mathbf{r})} = \mu_k \tag{67}$$

and the correlational counterpart yields

$$\frac{\delta F_c}{\delta\rho_k(\mathbf{r})} = -\frac{u_{kk}(0)}{2} - \frac{k_BT}{2}h_{kk}(\mathbf{r},\mathbf{r}). \tag{68}$$

If the excess chemical potential of a specie k is

$$\mu_k^{\rm ex} = \sum_{l}^{K}\rho_l^b\int d\mathbf{r}\,u_{kl}(r) - \frac{1}{2}\left[u_{kk}(0) + k_BTh_{kk}^b(0)\right], \tag{69}$$

then a density is

$$\rho_k(\mathbf{r}) = \rho_k^b e^{-\beta U_k(\mathbf{r})}e^{-\beta\sum_{l=1}^{K}\int d\mathbf{r}'(\rho_l(\mathbf{r}')-\rho_l^b)u_{kl}(\mathbf{r},\mathbf{r}')} \times e^{\frac{1}{2}[h_{kk}(\mathbf{r},\mathbf{r})-h_{kk}^b(0)]}. \tag{70}$$

B. Pressure

The pressure is obtained from the relation $P_{\rm ex} = \sum_{k=1}^{K} \rho_k^b \mu_k^{\rm ex} - f_{\rm ex}$, where the excess free-energy density in a bulk is

$$f_{\rm ex} = \frac{1}{2}\sum_{k,l}^{K} \rho_k^b \rho_l^b \int d\mathbf{r}\, u_{kl}(r) - \frac{1}{2}\sum_{k=1}^{K} \rho_k^b \left[u_{kk}(0) + k_B T \int_0^1 d\lambda\, \frac{h_{kk}^{b,\lambda}(0)}{\lambda} \right] \quad (71)$$

and includes the mean-field and correlational contributions. The excess pressure that results is

$$P_{\rm ex} = \frac{1}{2}\sum_{k,l}^{K} \rho_k^b \rho_l^b \int d\mathbf{r}\, u_{kl}(r) - \frac{k_B T}{2}\sum_{k=1}^{K} \rho_k^b \left[h_{kk}(0) - \int_0^1 d\lambda\, \frac{h_{kk}^{b,\lambda}(0)}{\lambda} \right]. \quad (72)$$

V. THE GAUSSIAN CORE MODEL

We apply the developed GRPA approximation to the Gaussian core model (GCM), whose pair interactions have the Gaussian functional form,

$$\beta u(r) = \varepsilon e^{-r^2/\sigma^2}, \quad (73)$$

where σ is the length scale that determines the interaction range and ε determines the interaction strength. Because at a complete overlap $\beta u(0) = \varepsilon$, particles are free to interpenetrate. The GCM is a theoretical invention of Stillinger [33–38] that found application as an effective interaction between polymers [39,40]. This started a more general interest in bounded potentials as a means for modeling various macromolecules encountered in soft matter [41]. An interesting feature of the GCM system is that, like water, it undergoes re-entrant melting when solid becomes too dense and the crystal arrangement can no longer be supported, triggering the melting transition.

For a homogenous system the free energy in Eq. (22) can be calculated exactly, and each individual ring term becomes

$$\mathrm{Tr}\, A^n = \frac{V(\varepsilon\eta_b)^n}{(n\pi\sigma^2)^{3/2}}, \quad (74)$$

where $\eta_b = \pi^{3/2}\sigma^3\rho_b$ is the reduced density and V is the volume of a system. The correlation free-energy density, $f_c = F_c/V$, becomes

$$f_c = \frac{\varepsilon\rho_b}{2}\sum_{n=2}^{\infty} \frac{(-\varepsilon\eta_b)^{n-1}}{n^{5/2}} = -\frac{\varepsilon\rho_b}{2}\left\{ 1 + \frac{\mathrm{Li}_{5/2}[-\varepsilon\eta_b]}{\varepsilon\eta_b} \right\}, \quad (75)$$

where $\mathrm{Li}_m(x) = \sum_{n=1}^{\infty} \frac{x^n}{n^m}$ is a polylogarithm.

Other quantities of interest follow. The excess chemical potential is

$$\beta\mu_{\rm ex} = \varepsilon\eta_b - \frac{\varepsilon}{2}\left\{ 1 + \frac{\mathrm{Li}_{3/2}[-\varepsilon\eta_b]}{\varepsilon\eta_b} \right\}. \quad (76)$$

Then, from comparison with Eq. (30), we get

$$h_b(0) = \varepsilon\sum_{n=1}^{\infty} \frac{(-1)^n(\varepsilon\eta_b)^{n-1}}{n^{3/2}} = \frac{\mathrm{Li}_{3/2}(-\varepsilon\eta_b)}{\eta_b}, \quad (77)$$

which then can be used to obtain pressure,

$$\frac{\beta P_{\rm ex}}{\rho_b} = \frac{\varepsilon}{2}\left\{ \eta_b + \frac{\mathrm{Li}_{5/2}(-\varepsilon\eta_b) - \mathrm{Li}_{3/2}(-\varepsilon\eta_b)}{\varepsilon\eta_b} \right\}. \quad (78)$$

Our primary interest, however, lies in the GRPA as a theory of inhomogeneous fluids. Considering a fluid confined by a hard wall to a half-space $x > 0$, we can use the contact value theorem to relate the pressure to a density at a contact with a wall,

$$\rho(0) = \beta P = \rho_b\left[1 + \frac{\varepsilon\eta_b}{2} + \frac{\mathrm{Li}_{5/2}(-\varepsilon\eta_b) - \mathrm{Li}_{3/2}(-\varepsilon\eta_b)}{2\eta_b} \right]. \quad (79)$$

The first term is the ideal-gas contribution, the second the mean-field contribution, and the last term accounts for the RPA correlations.

In Fig. 1 we compare the contact density at a wall as a function of ε for different approximations. The exact data points are from the MC simulation carried out for 1000 particles with periodic boundary conditions in three directions. The size of the box was modified to yield a desired bulk density ρ_b, and the pressure was calculated from the virial formula,

$$P = k_B T\rho_b - \frac{1}{3V}\sum_{i<j}^{N}\left\langle r_{ij}\frac{du(r_{ij})}{dr_{ij}} \right\rangle. \quad (80)$$

In general the RPA shows improvement over the mean field, except in the dilute limit, where both the mean-field and the RPA perform poorly. This is in agreement with the discussion in Sec. III E and not surprising if it is recalled that the RPA is designed as a correction over the mean field. In the dilute limit, the negative contributions of the RPA eventually bring the pressure down as a function of increased interactions. Again, this is predicted by Eq. (60) from which we also know that in the dilute limit $P_{\rm ex}$ becomes zero (the mean-field contribution is canceled by the RPA correlations leaving only the ideal gas part) for $\varepsilon = 4\sqrt{2} \approx 5.7$. For high densities the RPA appears accurate.

Figure 2 displays the direct correlation function for different approximations. The mean-field and the dilute limit curves are independent of a bulk density, and the GRPA curves, if accurate, should span between the two limiting cases as ρ_b changes from $0 \to \infty$. Indeed, in the limit $\rho_b \to \infty$ the GRPA converges to the mean-field but fails to converge to the correct behavior as $\rho_b \to 0$.

In Fig. 3 we plot the entire density profiles near a planar wall at $x = 0$. The improvement of the GRPA over the mean-field is visible not just near the wall but are noticeable in the far field.

In Fig. 4 we plot effective potentials due to the mean-field, $\beta U_{\rm eff}(x) = -\int d\mathbf{r}\,(\rho(x') - \rho_b)u(\mathbf{r},\mathbf{r}')$, and due to the RPA correlations, $\beta U_{\rm eff}(x) = -[h(x,x) - h_b(0)]/2$. The two potentials appear inverted. Near the wall the mean-field contributions are attractive, while the correlations contribute

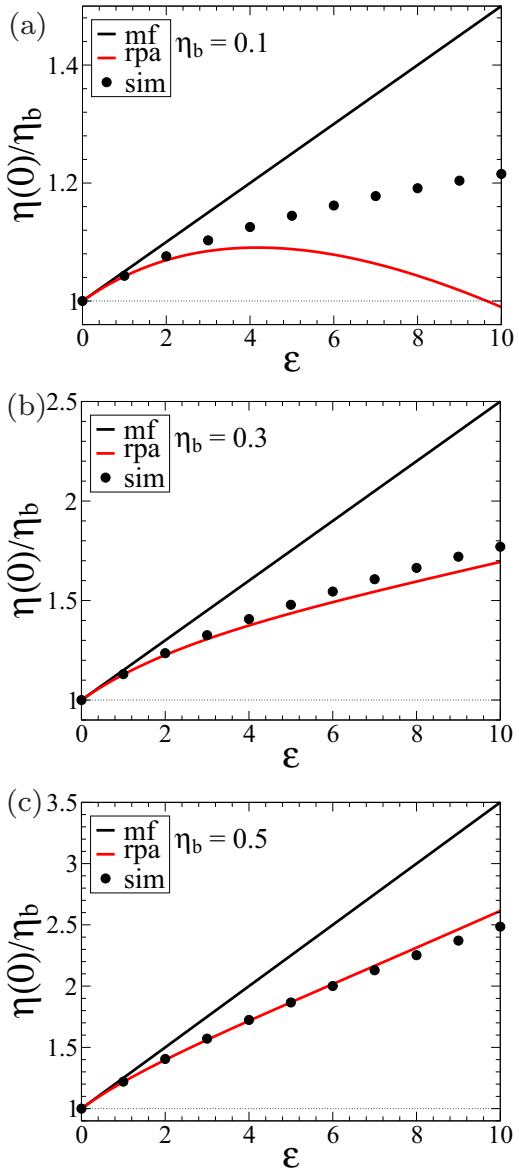

FIG. 1. The value of a density at a contact with a wall, $\eta(0) = \pi^{3/2}\sigma^3\rho(0)$, for a planar hard-wall model as a function of an interaction strength ε for a one component GCM. η_b is the bulk reduced density. The dotted horizontal line corresponds to an ideal-gas prediction. (a) $\eta_b = 0.1$; (b) $\eta_b = 0.3$; (c) $\eta_b = 0.5$.

repulsive interactions. The two potentials, furthermore, appear to have different oscillation wavelength.

VI. THE TWO-COMPONENT GCM

We next consider a two-component GCM fluid with interactions

$$u_{ij}(x) = \begin{cases} \varepsilon e^{-r^2/\sigma^2}, & \text{if } i = j \\ -\varepsilon e^{-r^2/\sigma^2}, & \text{if } i \neq j \end{cases}.$$

The reservoir concentration of both species is the same, $\rho_b = \rho_b^+ = \rho_b^-$, and the density profiles of both species are indistinguishable, in which case the mean-field contributions cancel out and the density profile is determined correlations

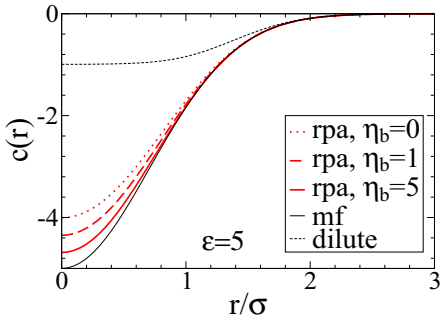

FIG. 2. Direct correlation function of a bulk fluid for the GCM model. The curves for the RPA are from Eq. (33), the mean-field curve is $c(r) = -\beta u(r)$, and the exact dilute limit is $c(r) = e^{-\beta u(r)} - 1$. Only the GRPA curves vary with density.

alone. The mean-field treatment (used in Refs. [13,32]) would predict a flat density profile for a wall model.

For a two-component fluid there are now four correlation functions $h_{kl}(\mathbf{r},\mathbf{r}')$: two same-species and two interspecies correlations. Within the GRPA all correlations are expressed through a single functional form,

$$h_{kl}(\mathbf{r},\mathbf{r}') = \begin{cases} h(\mathbf{r},\mathbf{r}') & \text{if } k = l \\ -h(\mathbf{r},\mathbf{r}') & \text{if } k \neq l \end{cases},$$

where $h(\mathbf{r},\mathbf{r}')$ is obtained from the OZ-RPA equation,

$$h(\mathbf{r},\mathbf{r}') = -\beta u(\mathbf{r},\mathbf{r}') - \beta \int d\mathbf{r}'' \rho(\mathbf{r}'') h(\mathbf{r}',\mathbf{r}'') u(\mathbf{r},\mathbf{r}''), \quad (81)$$

and $\rho(\mathbf{r}) = \rho_+(\mathbf{r}) + \rho_-(\mathbf{r})$ is the total density, and the correlation function is the same as for a one-component system. What differs is a density profile due to the absence of the mean-field contributions,

$$\rho(\mathbf{r}) = \rho_b e^{-\beta U(\mathbf{r})} e^{\frac{1}{2}[h(\mathbf{r},\mathbf{r}) - h_b(0)]}. \quad (82)$$

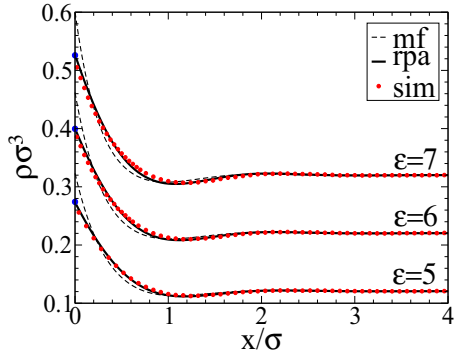

FIG. 3. Density profile for the GCM for the planar hard-wall model for different values of the interaction strength: $\varepsilon = 5,6,7$. A simulation box dimensions are $20\sigma : 20\sigma : 20\sigma$ and it contains 1000 particles. This roughly corresponds to a bulk density $\eta_b \approx 0.67$. The numerical data points for the mean field and the GRPA are for the same conditions. The filled blue circles at $x = 0$ are obtained from Eq. (79) to confirm accuracy of numerical results and the validity of the contact value theorem.

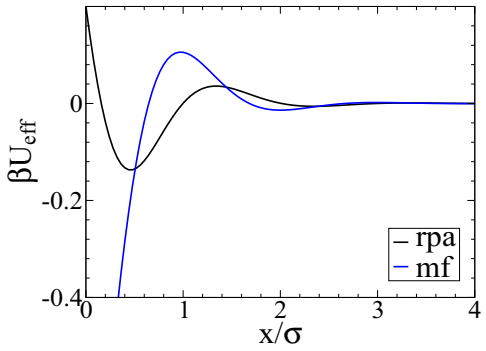

FIG. 4. Effective potentials due to the mean-field, $\beta U_{\rm eff} = -\int d\mathbf{r}\,[\rho(x') - \rho_b]u(\mathbf{r},\mathbf{r}')$, and the correlations, $\beta U_{\rm eff}(x) = -\frac{1}{2}[h(x,x) - h(0)]$ [see Eq. (31)], for a density profile in Fig. 3 with $\varepsilon = 7$.

For a bulk system, $h_b(0)$ is the same as in Eq. (77), while the pressure expression has no mean-field contributions,

$$\frac{\beta P_{\rm ex}}{\rho_b} = \frac{\varepsilon}{2}\left[\frac{\mathrm{Li}_{5/2}(-\varepsilon\eta_b) - \mathrm{Li}_{3/2}(-\varepsilon\eta_b)}{\varepsilon\eta_b}\right]. \tag{83}$$

Figure 5 displays the pressure (related to a contact density) as a function ε for different bulk densities. As density increases the accuracy of the GRPA breaks down. This differs from what we have seen for the one-component fluid where high density recovers the weakly correlated limit and the GRPA becomes more accurate. The flattening effect of exact curves is connected to pair formation (reminiscent of Bjerrum pairs in electrostatics) between different species. The poor performance of the GRPA for a two-component fluid at high density can therefore be seen as failure in predicting pairs.

In Fig. 6 we show an entire density profile of a two-component GCM fluid near a wall. The GRPA accurately predicts the depletion of particles from a wall region, since it is energetically unfavorable for a particle to be near a noninteractive wall than to be in a bulk surrounded by particles of other species. The exact results indicate a higher contact value, as well as a shift of an entire profile toward the wall, indicating that the depletion region is exaggerated by the GRPA.

VII. ONE-COMPONENT PLASMA

In this section we consider one-component Coulomb particles. The primary objective is to demonstrate that the GRPA equations transform to the expressions of a variational Gaussian approximation within the field-theoretical framework [23,24], without carrying out the Hubbard-Stratonovich transformation of the partition function.

Coulomb charges q interact via the following pair potential:

$$u(\mathbf{r},\mathbf{r}') = \frac{q^2}{4\pi\epsilon|\mathbf{r}-\mathbf{r}'|}, \tag{84}$$

where ϵ is the background dielectric constant. We re-emphasize that the divergence in $u(\mathbf{r},\mathbf{r}')$ as $\mathbf{r}\to\mathbf{r}'$ is not problematic as it is canceled by the divergence in $h(\mathbf{r},\mathbf{r}')$. To see this, revisit the expansion in Eq. (17).

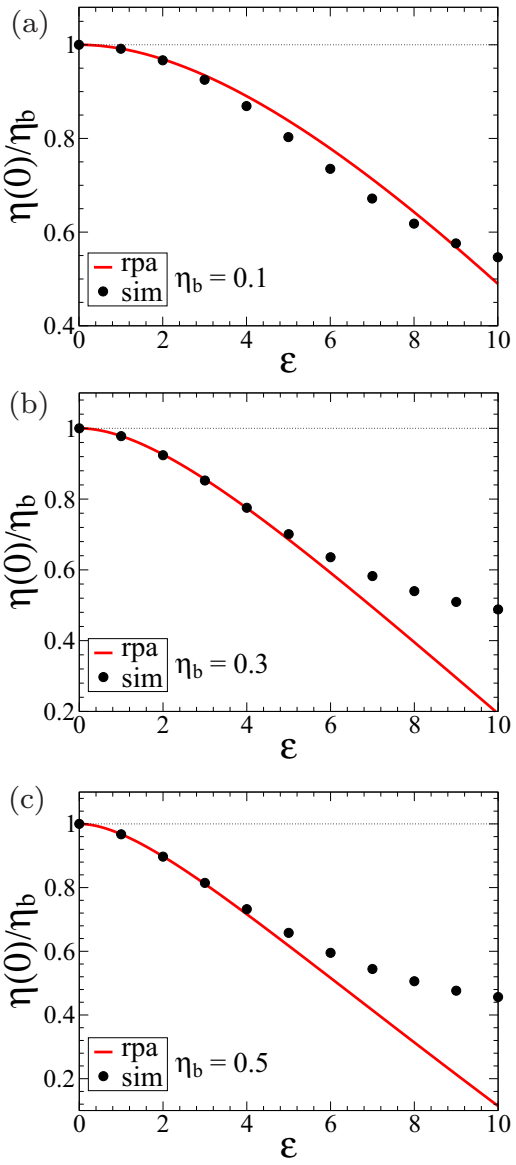

FIG. 5. The value of a density at a contact with a wall, $\eta(0) = \pi^{3/2}\sigma^3\rho(0)$, for a planar hard-wall model as a function of an interaction strength ε for a two-component GCM. η_b is the total reduced bulk density. The dotted horizontal line corresponds to an ideal-gas prediction. (a) $\eta_b = 0.1$; (b) $\eta_b = 0.3$; (c) $\eta_b = 0.5$.

A number density of Coulomb charges, using Eq. (31), is

$$\rho(\mathbf{r}) = \rho_b e^{-\beta q\psi(\mathbf{r})} e^{\frac{1}{2}[h(\mathbf{r},\mathbf{r}) - h_b(0)]}, \tag{85}$$

where the external potential, in electrostatic problems generated by permanent charges distributed over surfaces and accounted for by the boundary conditions, is omitted from the expression. Furthermore, we introduce an electrostatic potential $\psi(\mathbf{r})$ defined as

$$q\psi(\mathbf{r}) = \int d\mathbf{r}'\,\rho(\mathbf{r}')u(\mathbf{r},\mathbf{r}'). \tag{86}$$

To transform the OZ-RPA equation in Eq. (15) into desired form, we apply the Laplacian operator to both sides of the

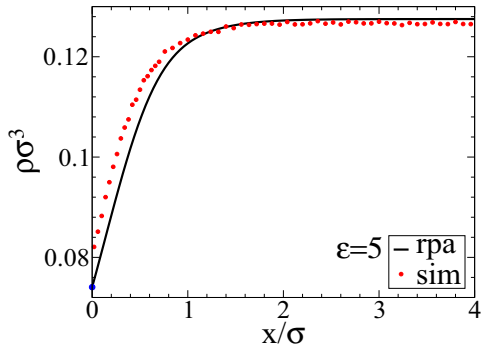

FIG. 6. A density profile for a two-component GCM fluid near a planar hard wall. The system size and the number of particles is the same as in Fig. 3.

equation,

$$\nabla^2 h(\mathbf{r},\mathbf{r}') = \frac{\beta q^2}{\epsilon}[\delta(\mathbf{r}-\mathbf{r}') + \rho(\mathbf{r})h(\mathbf{r},\mathbf{r}')], \tag{87}$$

where we used

$$\nabla^2 u(\mathbf{r},\mathbf{r}') = -\left(\frac{q^2}{\epsilon}\right)\delta(\mathbf{r}-\mathbf{r}'). \tag{88}$$

We carry out the same operation on Eq. (86),

$$\epsilon\nabla^2\psi(\mathbf{r}) = -q\rho(\mathbf{r}), \tag{89}$$

and the result is the standard Poisson equation.

Equations (85), (87), and (89) constitute the GRPA approximation for a density distribution and an electrostatic potential. To make contact with the variational equations of the field-theoretical framework the correlations in the number density $h(\mathbf{r},\mathbf{r}')$ need to be expresses as correlations in electrostatic potential. This can be done using a slightly rearranged OZ-RPA equation,

$$h(\mathbf{r},\mathbf{r}') = -\beta\int d\mathbf{r}''\,[\rho(\mathbf{r}'')h(\mathbf{r}',\mathbf{r}'') + \delta(\mathbf{r}'-\mathbf{r}'')]u(\mathbf{r},\mathbf{r}''). \tag{90}$$

The term $\rho(\mathbf{r}'')h(\mathbf{r}'',\mathbf{r}')$ in square brackets is a correlation hole generated when a single charge is fixed at $\mathbf{r}'$ and is represented by the δ function. The entire integral on the right-hand side can be regarded as a perturbation of an electrostatic potential, $\Psi(\mathbf{r},\mathbf{r}')$, caused by a fixed charge at $\mathbf{r}'$ [the total electrostatic potential is $\psi(\mathbf{r}) + \Psi(\mathbf{r},\mathbf{r}')$]. The OZ-RPA equation simply becomes

$$h(\mathbf{r},\mathbf{r}') = -\beta q\Psi(\mathbf{r},\mathbf{r}'), \tag{91}$$

and the proportionality between the two fluctuating quantities is established. Note that this is not an exact equality but a result specific within the GRPA.

We next consider a charged wall model and review some of the known results. For the wall model, there exists an analytical solution for the mean-field which corresponds to the weak-coupling limit. In the strong-coupling limit the density approaches an ideal-gas distribution [42,43]. The perturbative Gaussian correction to the mean-field has been considered in Refs. [22,44] and a semianalytical solution is available. The perturbative correction, however, fails to connect the weak- and strong-coupling limit and yields an unphysical "hump" near a wall for intermediate coupling parameters. Simulations, on the other hand, always show monotonically decreasing profile. We revisit the wall model to see if the variational Gaussian approximation (or the GRPA in our framework) is better in capturing the intermediate- and the strong-coupling limit. To our knowledge, this test has has not been done before.

We consider Coulomb particles with charge $q = e$. The wall surface charge is σ_c and the total system is neutral. The dielectric constant ϵ is the same on both sides of the wall. As the bulk density far away from the wall vanishes, the contact density is determined solely by the surface charge (not the pressure),

$$\rho(0) = -\int_0^\infty dz\,\rho(z)\frac{\partial U(z)}{\partial z} = \frac{\beta\sigma_c^2}{2\epsilon}, \tag{92}$$

where $-\partial U(z)/\partial z = -e\sigma_c/2$ is a constant force felt by particles on account of a uniform wall charge. The mean-field (or the Poisson-Boltzmann) solution is

$$\rho_{\rm mf}(x) = \frac{\beta\sigma_c^2}{2\epsilon}\left[\frac{1}{1+\beta q\sigma_c x/2\epsilon}\right]^2, \tag{93}$$

and it captures a weakly correlated limit. At the opposite end we have the strong-coupling limit where charges become distributed as ideal-gas particles [42,43],

$$\rho_{\rm sc}(x) = \frac{\beta\sigma_c^2}{2\epsilon}e^{-\beta q\sigma_c x/2\epsilon}. \tag{94}$$

A dimensionless parameter that determines the strength of correlations for the one-component system is taken to be the ratio between the Bjerrum and the Gouy-Chapman length, λ_B and $\lambda_D = 1/(2\pi\lambda_B\sigma_c)$, respectively, and is denoted as $\Xi = \lambda_B/\lambda_D$.

As correlations increase, the density evolves from one functional form to another, $\rho_{\rm mf} \to \rho_{\rm sc}$. A perturbative Gaussian approach for a counterion-only system yields a semi-analytic expression for a density correction $\Delta\rho(z)$, $\rho(z) = \rho_{\rm mf}(z) + \Delta\rho(z)$ [22,44], where $\int_0^\infty dz\,\Delta\rho(z) = 0$ in order to retain the neutrality, and $\Delta\rho(0) = 0$ so the contact value theorem remains satisfied. The corrected density develops a "hump" at a short distance from a wall leading to nonmonotonic behavior not confirmed by simulations, which always yield a monotonically decaying density.

We want to see if the GPRA (or variational Gaussian) proves a better approximation in representing the intermediate regime. The results are shown in Fig. 7. Unfortunately, they hardly differ from the perturbative approach. The "hump" is still there and it is not even reduced. The question is why the GRPA performs poorly for the one-component plasma or, more specifically, why correlations are exaggerated even for relatively low coupling constant $\Xi \approx 2$? To address this we note that the counterion-only system corresponds to a low-density fluid as the bulk density is zero, from the previous discussions and results we determined that the GRPA performs poorly in this limit.

To elucidate further the case of a one-component plasma, in Fig. 8 we plot an effective potential, $U_{\rm eff} = -\frac{1}{2}[h(x,x) - h_b(0)]$, of the perturbative Gaussian approximation of Refs. [22,44]. The potential is almost always attractive except just at the wall, where it suddenly rises leading to repulsive force that assures the satisfaction of the contact value theorem at the cost of an entire profile. Note also that the functional form

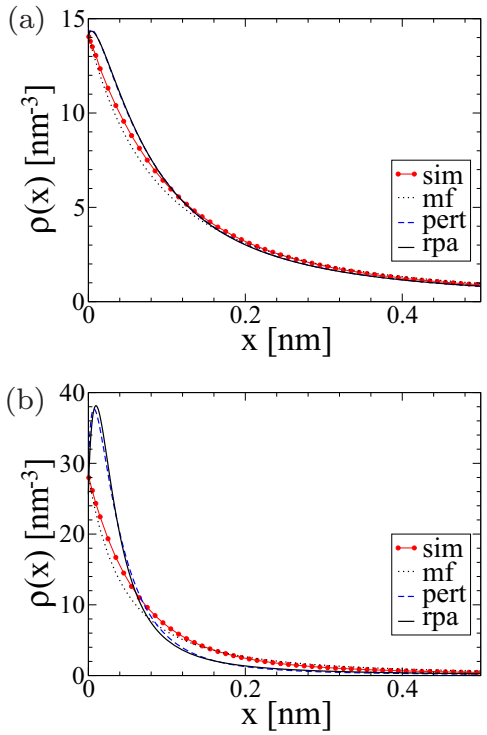

FIG. 7. Counterion density profiles for a counterion-only wall model. The surface charge density is $\sigma_c = 0.4$ C/m^2. For the Monte Carlo simulation we used the Ewalds summation for the periodic boundary conditions in the y and z directions. The simulation box contained 1000 particles and the size of the simulation box was $10 \times 10 \times 10$ nm. (a) $\lambda_B = 0.36$ nm, $\Xi = 2.03$; (b) $\lambda_B = 0.72$ nm $\Xi = 8.13$.

of the effective potential does not change and its magnitude is linear to the coupling constant Ξ. It is dubious that the weak- and strong-coupling limit should be governed by a single functional form.

VIII. ELECTROLYTE

We consider next a two-component plasma or an electrolyte. The primary objective, as for the case of a one-component plasma, is to demonstrate that the GRPA equations reduce to the variational Gaussian formulation within the field-theory framework. The variational Gaussian method was constructed specifically for Coulomb charges [23,24], whereas the present GRPA approach is general and applicable to any pair interactions, as was shown in its application to the Gaussian core model. To recover the variational Gaussian equations, the GRPA relations need to be re-expressed in terms of electrostatic potential, not the number density and its fluctuations.

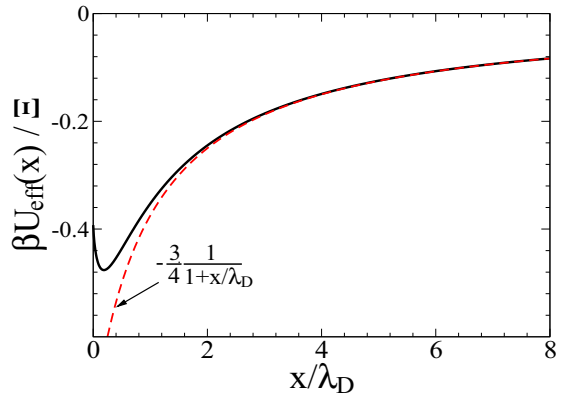

FIG. 8. Effective potentials due to correlations, $\beta U_{\rm eff}(x) = -\frac{1}{2}[h(x,x) - h(0)]$. Away from the wall $U_{\rm eff} = \frac{\Xi}{1+x/\lambda_D}$, where λ_D is the Guoy-Chapman length.

For a symmetric electrolyte $q:q$, pair interactions are

$$u_{kl}(\mathbf{r},\mathbf{r}') = \begin{cases} u(\mathbf{r},\mathbf{r}') & \text{if } k = l \\ -u(\mathbf{r},\mathbf{r}') & \text{if } k \neq l' \end{cases}$$

where $u(\mathbf{r},\mathbf{r}')$ is the Coulomb potential given in Eq. (84). The four correlation functions $h_{kl}(\mathbf{r},\mathbf{r}')$ between different species within the GRPA can be expressed in terms of a single function,

$$h_{kl}(\mathbf{r},\mathbf{r}') = \begin{cases} h(\mathbf{r},\mathbf{r}') & \text{if } k = l \\ -h(\mathbf{r},\mathbf{r}') & \text{if } k \neq l' \end{cases}$$

and $h(\mathbf{r},\mathbf{r}')$ is obtained from the OZ-RPA relation,

$$h(\mathbf{r},\mathbf{r}') = -\beta \int d\mathbf{r}'' \, [\rho(\mathbf{r}'')h(\mathbf{r}',\mathbf{r}'') + \delta(\mathbf{r}' - \mathbf{r}'')]u(\mathbf{r},\mathbf{r}''), \tag{95}$$

where $\rho(\mathbf{r}) = \rho_+(\mathbf{r}) + \rho_-(\mathbf{r})$ is the total density. Within the GRPA, the number density of each species is

$$\rho_\pm(\mathbf{r}) = \rho_b e^{\mp\beta q\psi(\mathbf{r})} e^{\frac{1}{2}[h(\mathbf{r},\mathbf{r}) - h_b(0)]}, \tag{96}$$

where the correlation function is obtained by transforming Eq. (95)

$$\epsilon\nabla^2 h(\mathbf{r},\mathbf{r}') = \beta q^2[\rho(\mathbf{r})h(\mathbf{r},\mathbf{r}') + \delta(\mathbf{r} - \mathbf{r}')]. \tag{97}$$

Finally, we still need the Poisson equation,

$$\epsilon\nabla^2\psi(\mathbf{r}) = -\rho_c(\mathbf{r}), \tag{98}$$

where $\rho_c(\mathbf{r}) = q\rho_+(\mathbf{r}) - q\rho_-(\mathbf{r})$ is a charge density. Equation (96), Eq. (97), and Eq. (98) constitute the GRPA approximation for a symmetric $q:q$ electrolyte.

In the final step in recovering the Gaussian variational equations the correlations in a number density are substituted by the correlations in electrostatic potential. We identify the term in brackets in Eq. (95) as a charge correlation hole generated by fixing either a positive or a negative charge q at $\mathbf{r}'$. For a fixed positive charge we have

$$\begin{aligned} \rho_{\rm hole}(\mathbf{r},\mathbf{r}') &= \rho_+(\mathbf{r})h_{++}(\mathbf{r},\mathbf{r}') - \rho_-(\mathbf{r})h_{+-}(\mathbf{r},\mathbf{r}') \\ &= \rho_+(\mathbf{r})h(\mathbf{r},\mathbf{r}') + \rho_-(\mathbf{r})h(\mathbf{r},\mathbf{r}') \\ &= \rho(\mathbf{r})h(\mathbf{r},\mathbf{r}'). \end{aligned} \tag{99}$$

The number density fluctuations can then be related to the fluctuations in electrostatic potential in a simple proportionality relation,

$$h(\mathbf{r},\mathbf{r}') = -\beta q\Psi(\mathbf{r},\mathbf{r}'), \tag{100}$$

as was already found in a one-component plasma in Eq. (91). Using this equality, Eq. (96) and Eq. (97) transform into the variational Gaussian equations within the field-theoretical framework [23,24].

We review some known results for homogenous electrolytes [45]. The excess chemical potential is

$$\mu_{\rm ex}^{\pm} = -\frac{1}{2}\lim_{r\to 0}[k_B T h_b(r) + u(r)], \tag{101}$$

and it depends exclusively on correlations as the mean-field contributions cancel out. The same is true of pressure,

$$P_{\rm ex} = -\frac{k_B T \rho_b}{2}\lim_{r\to 0}\left[h_b(r) - \int_0^1 d\lambda\, \frac{h_b^{\lambda}(r)}{\lambda}\right], \tag{102}$$

where $\rho_b = \rho_+^b + \rho_-^b$ is the bulk total density. To calculate the pressure we need to know correlations that we get from Eq. (97),

$$\frac{d^2 h_\lambda^b(r)}{dr^2} = \kappa_\lambda^2 h_\lambda^b(r) + \left(\frac{\lambda\beta q^2}{\epsilon}\right)\delta(r), \tag{103}$$

where $\kappa_\lambda = \sqrt{\lambda\beta q^2\rho_b/\epsilon}$ is the screening parameter, and the solution is the familiar Debye-Hückel solution,

$$h_b^{\lambda}(r) = -\frac{\lambda\beta q^2 e^{-\kappa_\lambda r}}{4\pi\epsilon r}, \tag{104}$$

and the excess pressure becomes

$$\beta P_{\rm ex} = -\frac{\kappa^3}{24\pi}, \tag{105}$$

where $\kappa \equiv \kappa_{\lambda=1}$.

For testing the GRPA approximation we consider a wall model without a surface charge and with the uniform dielectric constant across the interface. As the mean-field contributions vanish, the density depends on correlations alone,

$$\rho_\pm(\mathbf{r}) = \rho_b e^{\frac{1}{2}[h(\mathbf{r},\mathbf{r}) - h_b(0)]}. \tag{106}$$

The results are shown Fig. 9. The depletion layer near a wall is the result of correlations, not of the dielectric discontinuity as frequently is the case for interfaces. The depletion effect seen in Fig. 9 is driven by a solvation effect—ions prefer a bulk environment where they are surrounded by opposite charges while the vicinity of the wall impedes this arrangement. In summary, the GRPA overestimates the correlational contributions and becomes less accurate with increasing density.

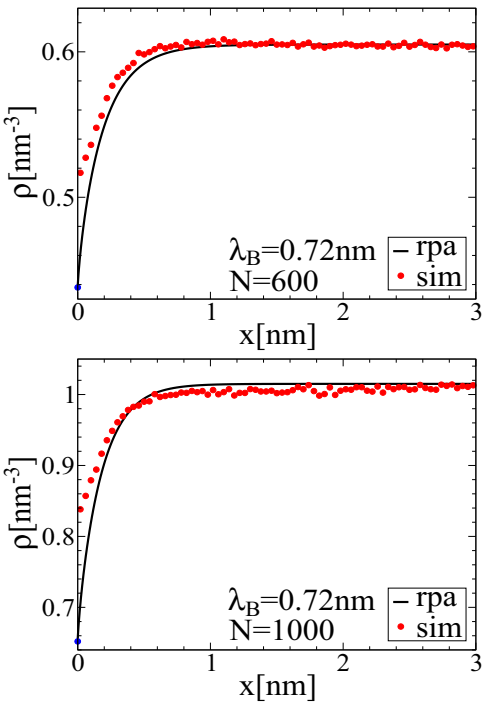

FIG. 9. Density profiles for a 1 : 1 electrolyte near a planar hard wall. MC simulations were carried out for $N = 600$ and $N = 1000$ particles, while the simulation box was fixed at $10 \times 10 \times 10$ nm. In the y and z direction we used Ewald summation to ensure the periodic boundary conditions. To make sure that the opposite charges do not collapse, the simulated ions are represented as charged hard spheres with diameter $\sigma = 0.2$ nm.

IX. CONCLUSION

The present work started out as a single-minded project of finding an alternative derivation for the variational Gaussian approximation, originally derived within the field-theoretical framework and intended specifically for Coulomb charges [23,24]. The motivation was, on the one hand, to be able to understand how the variational Gaussian method compares with liquid-state approaches, and, on the other hand, to find an alternative derivation of the relevant equations to bypass the heavy formalism of the field-theory and avoid various problems specific of that framework, such as the problem of divergences, invalidity of the Gibbs-Bogolyubov-Feynmann inequality in constructing the variational equations, impossibility to generalize the framework to an arbitrary pair potential [18].

By formulating the variational Gaussian approximation within a density-functional framework, we arrived at a generalized form of the RPA approximation [30]. Because, the derivation makes no assumptions about pair interactions, in principle, it is applicable to any system. (At first sight it may appear that the approximation is unsuitable for divergent potentials as a number of quantities depends on $u(0)$. But these divergences are always canceled by an identical divergence in the pair correlation function. For divergent potentials it makes more sense to write $\lim_{r\to 0} u(r)$).

We refer to the present RPA density-functional framework as the GRPA to distinguish it from the RPA method applied to the GCM fluid [13,32] and that in the present work we refer to as the mean-field. We verified that within the GRPA framework, different definitions of pressure (the "compressibility" and "virial" expressions) yield the same result and that the GRPA satisfies the contact value theorem sum rule, proving the GRPA to be a consistent framework.

Intended as the correction to the mean-field, the GRPA shares similar drawbacks as the mean-field. In consequence, it is not a low-density approximation and the designed function is not intended to recover the exact dilute limit behavior. The situation is more subtle for two-component systems where the mean-field contributions vanish altogether and the correlations constitute the sole contributions beyond those of the ideal gas. In that case, the larger density does not imply more accurate predictions. Large density produces, in fact, consistently

poorer results. We attribute this behavior to failure of the GRPA to predict pair formation between opposite species, reminiscent of Bjerrum pairs in electrolytes. In order to predict correct phase diagram of an electrolyte, Bjerrum pairs had to be put "by hand," in addition to the GRPA type of correlations (obtained through the Debye charging process) [46]. This implies that one needs to include contributions beyond the GRPA for a more efficient description of dense two-component systems with propensity to pair formation.

With growing number of soft-matter systems involving diverse effective interactions [47,48], the GRPA could potentially find use as a general theoretical framework for dealing with these novel systems. Up to now, the best theories are for hard-spheres while the mean-field is used for all the rest. But there are still challenges ahead. The first challenge is to understand the limits of the GRPA and the conditions under which it is reliable. Another part of the challange is technical and is concerned with actual implementation. The fundamental measure DFT owes its success to its easy implementation and robust computation. If the GRPA could be reduced to the similar level of computational effort as the mean-field, then it would indeed become an attractive theoretical tool. The technical difficulty of the GRPA is the computation of operators A^n, and their traces $\mathrm{Tr}\, A^n$ (or ring diagrams). For example, we see in Eq. (38) how a thermodynamic integral can be represented in terms of ring diagrams. These operators constitute the basic building blocks of the method and their computation requires different approach than that for the fundamental measure DFT based on weighted densities and their functions. At this point, it is still difficult to say how useful the GRPA can be in the future. As of now, it is just an alternative derivation of the variational Gaussian approximation with potential for broader applications.

ACKNOWLEDGMENTS

Most computations were done by machines in the Laboratoire de Physico-Chime Théorique, ESPCI, with the generous permission and assistance of Tony Maggs and Michael Schindler. D.F. would like to thank Tony Maggs for discussions regarding implementation of the GRPA and Yan Levin for reading the manuscript. This research was partly supported by the National Natural Science Foundation of China, Grant No. 11574198.

[1] R. Evans, Adv. Phys. A **28**, 143 (1979).
[2] Y. Rosenfeld, Phys. Rev. Lett. **63**, 980 (1989).
[3] P. Tarazona, J. A. Cuesta, and Y. Martínez-Ratón, Lect. Notes Phys. **753**, 247 (2008).
[4] R. Evans, *Lecture Notes at 3rd Warsaw School of Statistical Physics* (Warsaw University Press, Kazimierz Dolny, 2009), p. 4385.
[5] R. Roth, J. Phys.: Condens. Matter **22**, 063102 (2010).
[6] D. Frydel and Y. Levin, J. Chem. Phys. **137**, 164703 (2012).
[7] J. A. Barker and D. Henderson, J. Chem. Phys. **47**, 2856 (1967).
[8] M. Schmidt, J. Phys.: Condens. Matter **11**, 10163 (1999).
[9] M. Schmidt, Phys. Rev. E **60**, R6291 (1999).
[10] M. Schmidt, Phys. Rev. E **62**, 4976 (2000).
[11] H. Löwen, J. Phys.: Condens. Matter **14**, 11897 (2002).
[12] M B Sweatman, J. Phys.: Condens. Matter **14**, 11921 (2002).
[13] A. A. Louis, P. G. Bolhuis, and J. P. Hansen, Phys. Rev. E **62**, 7961 (2000).
[14] A. Abrashkin, D. Andelman, and H. Orland, Phys. Rev. Lett. **99**, 077801 (2007).
[15] D. Frydel, J. Chem. Phys. **134**, 234704 (2011).
[16] D. Frydel and Y. Levin, J. Chem. Phys. **138**, 174901 (2013).
[17] D. Frydel, Adv. Chem. Phys. **160**, 209 (2016).
[18] D. Frydel, Eur. J. Phys. **36**, 065050 (2015).
[19] R. Podgornik and B. Zeks, J. Chem. Soc., Faraday Trans. 2 **84**, 611 (1988).
[20] P. Attard, D. J. Mitchell, and B. W. Ninham, J. Chem. Phys. **88**, 4987 (1988).
[21] R. D. Coalson and A. Duncan, J. Chem. Phys. **97**, 5653 (1992).
[22] R. R. Netz and H. Orland, Eur. Phys. J. E **1**, 67 (2000).
[23] R. Netz and H. Orland, Eur. Phys. J. E **11**, 301 (2003).
[24] Z.-G. Wang, Phys. Rev. E **81**, 021501 (2010).
[25] P. Duncan, M. M. Hatlo, and L. Lue, A field-theory approach for modeling electrostatic interactions in soft matter, in *Proceedings of the CECAM Workshop New Challenges in Electrostatics of Soft and Disordered Matter* (Pan Stanford, Singapore, 2014).
[26] Zhenli Xu and A. C. Maggs, J. Comp. Phys. **275**, 310 (2014).
[27] D. Pines and D. Bohm, Phys. Rev. **85**, 338 (1952).
[28] M. Gell-Mann and K. A. Brueckner, Phys. Rev. **106**, 364 (1957).
[29] J. P. Perdew and D. C. Langreth, Phys. Rev. B **15**, 2884 (1977).
[30] X. Ren, P. Rinke, C. Joas, and M. Scheffler, J. Mater. Sci. **47**, 7447 (2012).
[31] J. P. Hansen and I. R. McDonald, *Theory of Simple Fluids* (Academic Press, London, 2005).
[32] A. J. Archer and R. Evans, Phys. Rev. E **64**, 041501 (2001).
[33] F. H. Stillinger, J. Chem. Phys. **65**, 3968 (1976).
[34] F. H. Stillinger and T. A. Weber, J. Chem. Phys. **68**, 3837 (1978).
[35] F. H. Stillinger and T. A. Weber, Phys. Rev. B **22**, 3790 (1980).
[36] F. H. Stillinger, J. Chem. Phys. **70**, 4067 (1979).
[37] F. H. Stillinger, Phys. Rev. B **20**, 299 (1979).
[38] F. H. Stillinger and D. K. Stillinger, Physica A **244**, 358 (1997).
[39] P. J. Flory and W. Krigbaum, J. Chem. Phys. **18**, 1086 (1950).
[40] A. A. Louis, P. G. Bolhuis, J. P. Hansen, and E. J. Meijer, Phys. Rev. Lett. **85**, 2522 (2000).
[41] C. N. Likos, A. Lang, M. Watzlawek, and H. Löwen, Phys. Rev. E **63**, 031206 (2001).
[42] A. G. Moreira and R. R. Netz, Europhys. Lett. **52**, 705 (2000).
[43] L. Ŝamaj and E. Trizac, Phys. Rev. Lett. **106**, 078301 (2011).
[44] L. Ŝamaj, Eur. Phys. J. E **36**, 100 (2013).
[45] Y. Levin, Rep. Prog. Phys. **65**, 1577 (2002).
[46] M. E. Fisher and Y. Levin, Phys. Rev. Lett. **71**, 3826 (1993).
[47] C. N. Likos, Phys. Rep. **348**, 267 (2001).
[48] C. N. Likos, Soft Matter **2**, 478 (2006).